JNCI J Natl Cancer Inst (2015) 107(4): dju504

doi:10.1093/jnci/dju504
First published online February 18, 2015
Article

ARTICLE

Combined Treatment Strategies for Microtubule Stabilizing Agent-Resistant Tumors

Angela Broggini-Tenzer, Ashish Sharma, Katarzyna J. Nytko, Sabine Bender, Van Vuong, Katrin Orlowski, Daniel Hug, Terence O'Reilly, Martin Pruschy

Affiliations of authors: Laboratory for Molecular Radiobiology, Radiation Oncology, University Hospital Zurich, Zurich, Switzerland (ABT, AS, KJN, SB, VV, KO, DH, TOR, MP); Department of Dermatology, University Hospital Zurich, Zurich, Switzerland (DH); Clinical Research Priority Program Tumor Oxygenation, University Hospital Zurich, Zurich, Switzerland (KJN, MP).

Current affiliation: Novartis Pharma Switzerland (KO).

Correspondence to: Martin Pruschy, PhD, Department of Radiation Oncology, University Hospital Zurich, CH-8091 Zurich, Switzerland (e-mail: martin.pruschy@usz.ch).

Abstract

Background: Resistance to microtubule-stabilizing agents is a major hurdle for successful cancer therapy. We investigated combined treatment of microtubule-stabilizing agents (MSAs) with inhibitors of angiogenesis to overcome MSA resistance.

Methods: Treatment regimens of clinically relevant MSAs (patupilone and paclitaxel) and antiangiogenic agents (everolimus and bevacizumab) were investigated in genetically defined MSA-resistant lung (A549EpoB40) and colon adenocarcinoma (SW480) tumor xenografts in nude mice (CD1-Foxn1<nu>, ICRnu; 5–14 per group). Tumor growth delays were calculated by Kaplan-Meier analysis with Holm-Sidak tests. All statistical tests were two-sided.

Results: Inhibition of mTOR-kinase by everolimus only minimally reduced the proliferative activity of β tubulin–mutated lung adenocarcinoma cells alone and in combination with the MSA patupilone, but everolimus inhibited expression and secretion of vascular endothelial growth factor (VEGF) from these cells. mTOR-kinase inhibition strongly sensitized tumor xenografts derived from these otherwise MSA-resistant tumor cells to patupilone. Tumors treated with the combined modality of everolimus and patupilone had statistically significantly reduced tumor volume and stronger tumor growth delay (16.2 ± 1.01 days) than control- (7.7 ± 0.3 days, $P = .004$), patupilone- (10 ± 0.97 days, $P = .009$), and everolimus-treated (10.6 ± 1.4 days, $P = .014$) tumors. A combined treatment modality with bevacizumab also resensitized this MSA-refractory tumor model to patupilone. Treatment combination also strongly reduced microvessel density, corroborating the relevance of VEGF targeting for the known antivasculature-directed potency of MSA alone in MSA-sensitive tumor models. Resensitization to MSAs was also probed in P glycoprotein–overexpressing SW480-derived tumor xenografts. Different bevacizumab regimens also sensitized this otherwise-resistant tumor model to clinically relevant MSA paclitaxel.

Conclusions: A treatment combination of MSAs with antiangiogenic agents is potent to overcome tumor cell–linked MSA resistance and should be considered as strategy for MSA-refractory tumor entities.

Microtubule-stabilizing agents (MSAs) belong to the most important classes of anticancer agents. Preventing the shortening of microtubules, they interfere with the dynamics of the microtubular network, which results in a transient or permanent M-phase arrest and the induction of apoptotic cell death or mitotic catastrophe (1–4).

Received: March 13, 2014; **Revised:** October 12, 2014; **Accepted:** December 19, 2014

© The Author 2015. Published by Oxford University Press. All rights reserved. For Permissions, please e-mail: journals.permissions@oup.com.

Taxanes and epothilones are the clinically most relevant microtubule-stabilizing agents. Taxanes have been approved for a broad range of indications, including advanced breast cancer after failure of combination chemotherapy or at early relapse (5), high-grade ovarian cancer in combination with platinum compounds, and primary treatment of non–small cell lung cancer in combination with cisplatin or carboplatin (6). Epothilones, which are structurally distinct from taxanes, may overcome some of their limitations suggesting a promising new treatment approach for cancer (7–9). Epothilones share the same binding site on β-tubulin with taxanes, albeit with different affinities and a slightly distinct mechanism of action. Several properties like increased water solubility, low susceptibility to common mechanisms of resistance, and the more tolerable toxicity profile favor their development (10). Ixabepilone (Ixempra, Bristol Myers-Squibb) is the first approved compound in this class and is indicated as monotherapy or in combination with capecitabine for the treatment of patients with metastatic breast cancer (11).

Resistance to paclitaxel is linked to altered cellular β-tubulin isotype composition (12) and β tubulin–related mutations, which have been identified in tumor cell lines but also in the patient situation (13,14). A major clinical hurdle represents tumor-associated high expression of P glycoprotein–related multidrug resistance (MDR), which limits broad range application of taxanes, but not of epothilones (10).

Tumor cells are the primary targets for classic anticancer treatment. Apart from their direct tumor cell–directed cytotoxicity, MSAs are also antiangiogenic and show antivascular effects (15–19). We and others previously demonstrated that MSAs downregulate the hypoxia-inducible factor (HIF)–transcriptome and interfere with the secretion of multiple tumor cell–derived factors, eg, the major endothelial cell survival factor vascular endothelial growth factor (VEGF) and stress-induced tissue inhibitors of matrix metalloproteinase (TIMP) (20–23). Thus, the tumor growth–inhibitory effect of MSAs in MSA-sensitive tumors might at least in part be because of their indirect, tumor cell–mediated effect on the tumor microenvironment.

The combined treatment modality of MSAs in combination with antiangiogenic agents was investigated in vitro and in vivo in preclinical MSA-sensitive tumor systems (24–29). At the same time, several clinical trials are ongoing combining different classes of MSAs with inhibitors of angiogenesis (25,28,30). However, such a combined treatment modality might also represent an approach to overcome a tumor cell–linked treatment resistance to MSAs. Here we investigate a rationally designed combined treatment approach to overcome MSA resistances related to two distinct genetically defined resistance mechanisms demonstrating that the microenvironment strongly determines the treatment response.

ARTICLE

Methods

Compounds and Cell Cultures

Patupilone (epothilone B, EPO906) and Everolimus (RAD001) were provided by Novartis Pharma (Basel, Switzerland). For in vitro experiments, patupilone and everolimus were dissolved in DMSO (1 mM stock solution) and further diluted in serum-containing medium. VEGF (Sigma, #V7259) was dissolved in H_2O (1 mg/mL) and further diluted in serum-containing medium. A549, A549EpoB40, and SW480 cells were grown in RPMI 1640 containing 10% fetal bovine serum, 1% penicillin-streptomycin, and 2 mM L-glutamine at 37°C in 5% CO_2. Genotyped A549 and A549EpoB40 cells were a gift from Susan Band Horwitz (Albert Einstein College of Medicine, NY) and phenotypically tested for patupilone sensitivity. SW480 cells were obtained from ATCC. Human umbilical vein cells (HUVECs) were cultured in endothelial growth medium (Promo Cell, #C-22210), supplemented with growth factors (PromoCell, C-39210#), 1% penicillin-streptomycin at 37°C in 5% CO_2.

Cell Proliferation Assay and Western Blot Analysis

The proliferative activity of tumor and endothelial cells was assessed with the colorimetric alamarBlue assay as described in detail in (15). Four western blot analysis cells were incubated for 24 hours and one hour with patupilone and everolimus, respectively, followed by incubation under normoxic or hypoxic conditions (0.2% pO2; Invivo2 400 hypoxia workstation, Biotrace International, Bridgend, UK) and cell lysis in lysis buffer (63mM Tris, 10% Glycerol, 2% SDS, pH 6.8 + DTT) and SDS-PAGE. Antibody detection was achieved by enhanced chemoluminescence (Amersham, Piscataway, NJ) using a polyclonal rabbit anti–HIF-1α subunit antibody (Santa Cruz Biotechnology, #sc-10790, 1:1000), a rabbit polyclonal anti–phospho-P70-S6kinase antibody (Cell Signalling Technology, #9205, 1:1000), a rabbit polyclonal anti–P70-S6kinase antibody (Cell Signalling Technology, #9202, 1:1000) and a mouse monoclonal anti–β-actin antibody (Sigma Aldrich, #A5441, 1:1000). All experiments were carried out independently at least three times.

RNA Extraction and Quantitative Real-Time Polymerase Chain Reaction

Sample RNA was isolated using an RNeasy Mini Kit (Qiagen) followed by reverse transcription and cDNA amplification using a High Capacity cDNA Reverse Transcription Kit (Applied Biosystems), and a FastStart Universal SYBR Green Master Mix (Roche) on an Applied Biosystems 7900HT real-time polymerase chain reaction instrument. Gene expression values represent $2^{-\Delta\Delta Ct}$, normalized to GAPDH mRNA. The primers used were: VEGFA 5`-GAAGTGGTGAAGTTCATGGATGTCTAT-3` (forward) and 5`-TCAGGGTACTCCTGGAAGATGTC-3` (reverse), GAPDH 5`- ACCC ACTCCTCCACCTTT-3` (forward), and 5`-CTCTTGTGCTCT TGC TGG-3` (reverse). All assays were performed in triplicates.

Enzyme-Linked Immunosorbent Assay

The concentration of VEGF levels in the filtered, conditioned media of A549EpoB40 cells was determined using the Quantikine Human VEGF Immunoassay kit (R&D Systems GmbH).

Tumor Xenografts

Tumor xenografts derived from A549, A549EpoB40, and SW480 cells in athymic nude mice (5–14 per group) were generated as described in (15) and allowed to expand to a volume of 200 mm^3 (±10%) before treatment start and random assignment. Patupilone (EPO906) was dissolved in 30% PEG-300/70% saline, and a single dose was applied intravenously at 2 mg/kg. Everolimus was diluted in 5% sucrose solution and administered p.o. at 2.5 mg/kg during five consecutive days. Bevacizumab (Avastin, Roche, concentrated infusion solution) was diluted

with saline and injected i.p. at 10 mg/kg twice (SW480) or three times (A549EpoB40). Paclitaxel (Taxol, Bristol-Myers Squibb, concentrated infusion solution) was diluted with saline and injected i.p. at 20 mg/kg. Control mice received a corresponding placebo treatment. This study was performed in strict accordance with the recommendations in the Guide for the Care and Use of Laboratory Animals of the Swiss Cantonal Veterinary Authorities.

Histology

Immunohistological endpoints were assessed as described in (15) for Ki-67 (rabbit clone SP6; dilution 1:100; NeoMarkers, Fremont, CA), CD31 (rabbit polyclonal, ab28364; dilution 1:50; Abcam, Cambridge, UK), and phospho-P70-S6Kinase (Cell Signalling Technology, #9202), using a Discovery immunohistochemistry staining system (Ventana Medical Systems). Phospho-P70-S6Kinase and Ki-67–positive tumor cells and amount of vessels (CD31) were counted in at least three randomly chosen visual fields (magnification 800x, 0.16mm^2) in each xenograft (n = 3 for each group).

Statistical Analysis

In vitro data (VEGF expression and secretion analysis) were analyzed by one-way analysis of variance (ANOVA) on replicate data. Pair-wise analyses were performed using the Tukey Test with relevant comparisons given in the text. Two different metrics were used to analyze in vivo treatment response data. Areas under the tumor volume curve (AUCs) were analyzed either by one-way ANOVA using the Tukey Test for pair-wise comparisons or ANOVA on ranks with the Dunn Test for pair-wise comparison. Additionally, tumor growth delays were calculated by Kaplan-Meier analysis with Holm-Sidak tests being used for pair-wise comparisons. Immunohistochemical data were analyzed by one-way ANOVA on replicate tumor samples (n = 6–9), and pair-wise analysis was performed using the Tukey Test. Relevant comparisons are given in the text and figures. All statistical tests were two-sided.

Results

We and others previously demonstrated that MSAs downregulate the HIF transcriptome and interfere with the secretion of multiple tumor cell–derived factors, eg, VEGF (20,21,23). The MSA-resistant A549EpoB40-derived tumor xenograft model was used to probe resensitization by interference with tumor-derived growth factor secretion. A549EpoB40 cells contain a defined β-tubulin mutation and are up to 100 fold more resistant to classic MSAs such as epothilones and taxanes in comparison with their wild-type counterpart cells (A549) (8,15,31).

To probe VEGF expression and secretion in response to patupilone, A549EpoB40 cells were treated for 24 hours with patupilone at a concentration (0.2 nM) that was previously shown to downregulate the HIF transcriptome and subsequent VEGF expression in the corresponding A549 wild-type cells (15,23). As expected, VEGF expression and secretion was enhanced when A549EpoB40cells were kept under hypoxic conditions, but patupilone treatment did not affect VEGF expression and VEGF secretion under normoxic and hypoxic conditions in these MSA-resistant cells (Figure 1, A and B).

Clinically relevant mTOR inhibitors decrease the expression and secretion of tumor-derived VEGF by inhibition of the mTOR-controlled HIF signal transduction cascade. The effect of the environment on VEGF expression and secretion was profound (normoxia vs hypoxia, $P < .001$). In contrast to patupilone, the mTOR inhibitor everolimus potently reduced VEGF expression and secretion under both environmental conditions in A549EpoB40 cells (normoxia, controls vs everolimus, $P < .001$; hypoxia, controls vs everolimus, $P < .001$). Combined treatment with everolimus and patupilone reduced VEGF production as compared with controls but was not statistically different from everolimus treatment alone (Figure 1, A and B). Probing the activity of the mTOR downstream target P70-S6kinase demonstrated that everolimus but not patupilone potently inhibited mTOR activity under these conditions. In line with these results, hypoxia-dependent stabilization of the HIF-1α subunit was strongly counteracted in everolimus- but not in patupilone-treated MSA-resistant A549EpoB40 cells (Figure 1C).

Effect of Patupilone, Everolimus, and Combined Treatment on Growth of A549EpoB40-Derived Tumor Xenografts

In vitro control experiments revealed that A549EpoB40 tumor cells were completely resistant to patupilone at a concentration (0.5 nM) that strongly reduced the proliferative capacity in A549 wild-type and other carcinoma cell lines (Figure 2A) (15). Treatment of A549EpoB40 cells with everolimus partially reduced their proliferative capacity at a concentration that strongly inhibited mTOR activity (2.5 nM) (Figure 1C). However, no additive antiproliferative effect could be observed on combined treatment with patupilone (Figure 2A). To determine the treatment response to patupilone and everolimus alone and sensitization to patupilone as part of a combined treatment modality in vivo, mice with A549EpoB40-derived MSA-resistant tumor xenografts were treated with everolimus (2.5 mg/kg/day) during five consecutive days and a single dose of patupilone (2 mg/kg, day 3) alone and in combination. Patupilone did not induce any growth inhibitory response in A549EpoB40-derived tumors (Figure 2B). Treatment with everolimus resulted in a minor but again not statistically significant change in tumor volume area under the curve (AUC) and tumor growth delay. Interestingly though, this minimal combined treatment regimen of patupilone and everolimus resulted in a statistically significant reduction of AUC in these otherwise patupilone-resistant tumors (combined 6317 ± 360 vs control 9525 ± 186, $P < .05$) (Figure 2B). Five out of six tumors treated with the combined treatment modality did not triple the initial tumor volume by the end of the observation time, demonstrating a potent and prolonged combined treatment effect of patupilone and everolimus. Likewise a statistically significant tumor growth delay could also be observed at smaller tumor volumes. At the target tumor volume of 400 mm^3, tumors treated with the combined modality of everolimus and patupilone had a statistically significantly stronger tumor growth delay (16.2 ± 1.01 days) than control- (7.7 ± 0.3 days, $P = .004$), patupilone- (10 ± 0.97 days, $P = .009$), and everolimus-treated (10.6 ± 1.4 days, $P = .014$) tumors, respectively, suggesting a positive interaction between patupilone and everolimus (Figure 2C). Lack of a strong (supra)-additive effect in vitro corroborates that the treatment combination in vivo derives from an interplay between the tumor cell compartment and the tumor microenvironment.

The combined treatment modality of patupilone and everolimus was probed in parallel in tumors derived from β-tubulin wild-type A549 lung adenocarcinoma cells. These tumors showed increased sensitivity to everolimus, but more important

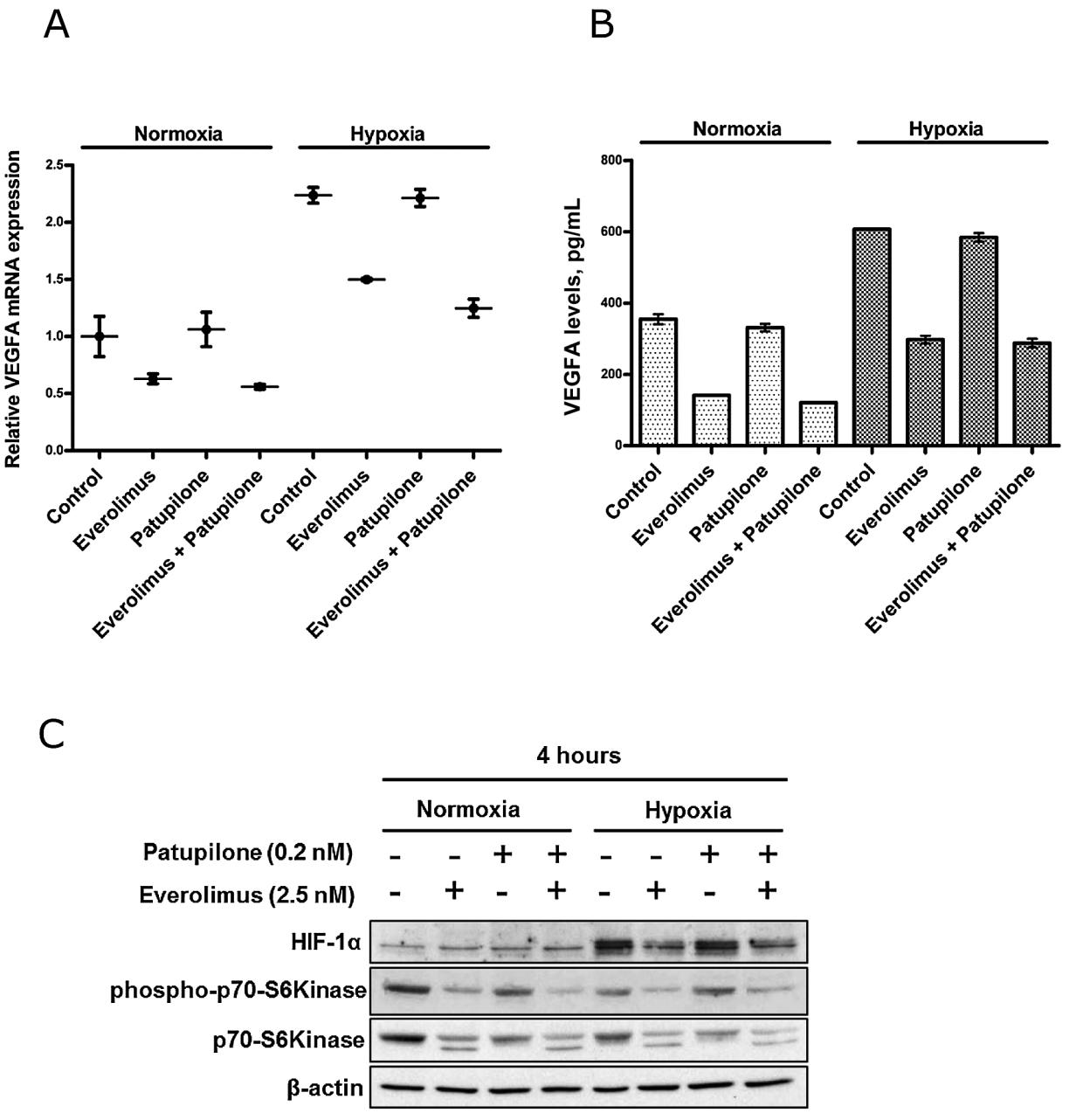

Figure 1. Regulation of vascular endothelial growth factor (VEGF)–mRNA-expression **(A)** and VEGF secretion **(B)** by patupilone and everolimus. A549EpoB40 cells were treated with patupilone (0.2 nM, 24 hours) and/or everolimus (2.5 nM, one hour) and cultured under normoxic and hypoxic (0.2%) conditions. VEGF mRNA was determined 24 hours after starting hypoxic conditions by real-time polymerase chain reaction. Supernatants were collected and analyzed for VEGF protein levels by enzyme-linked immunosorbent assay. Data are means of at least three independent experiments. **Error bars** represent standard deviations. **C)** Patupilone- and everolimus-treated A549EpoB40 cell lysates were tested against the phosphorylated form of p70-S6Kinase and HIF-1α subunit by western blotting. Cells were preincubated with patupilone and everolimus for half an hour followed by additional incubation for four hours under normoxic or hypoxic conditions and cell lysis. Picture shows one representative experiment out of three experiments.

patupilone alone already induced a strong tumor growth delay, which was not further enhanced by the combined treatment with everolimus (Supplementary Figure 1, available online).

Effect of Patupilone, Bevacizumab, and Combined Treatment on Growth of A549EpoB40-Derived Tumor Xenografts

Downregulation of the HIF-transcriptome with subsequent reduction of tumor-derived VEGF expression could be executed by the mTOR inhibitor everolimus instead of patupilone in MSA-resistant tumors (23,32). However, the mTOR inhibitor could also directly target endothelial cells. To specifically investigate the relevance of VEGF for resensitization of MSA-resistant tumors to patupilone, mice carrying tumor xenografts derived from A549EpoB40 cells were treated with patupilone in combination with the αVEGF-inhibitory antibody bevacizumab. In vitro control experiments revealed that the proliferative capacity of A549EpoB40 tumor cells was also not affected by patupilone and bevacizumab alone and in combination (Figure 3A). A549EpoB40-derived tumors were completely resistant to patupilone (1x2 mg/kg, day 3), whereas bevacizumab (3x10 mg/kg,

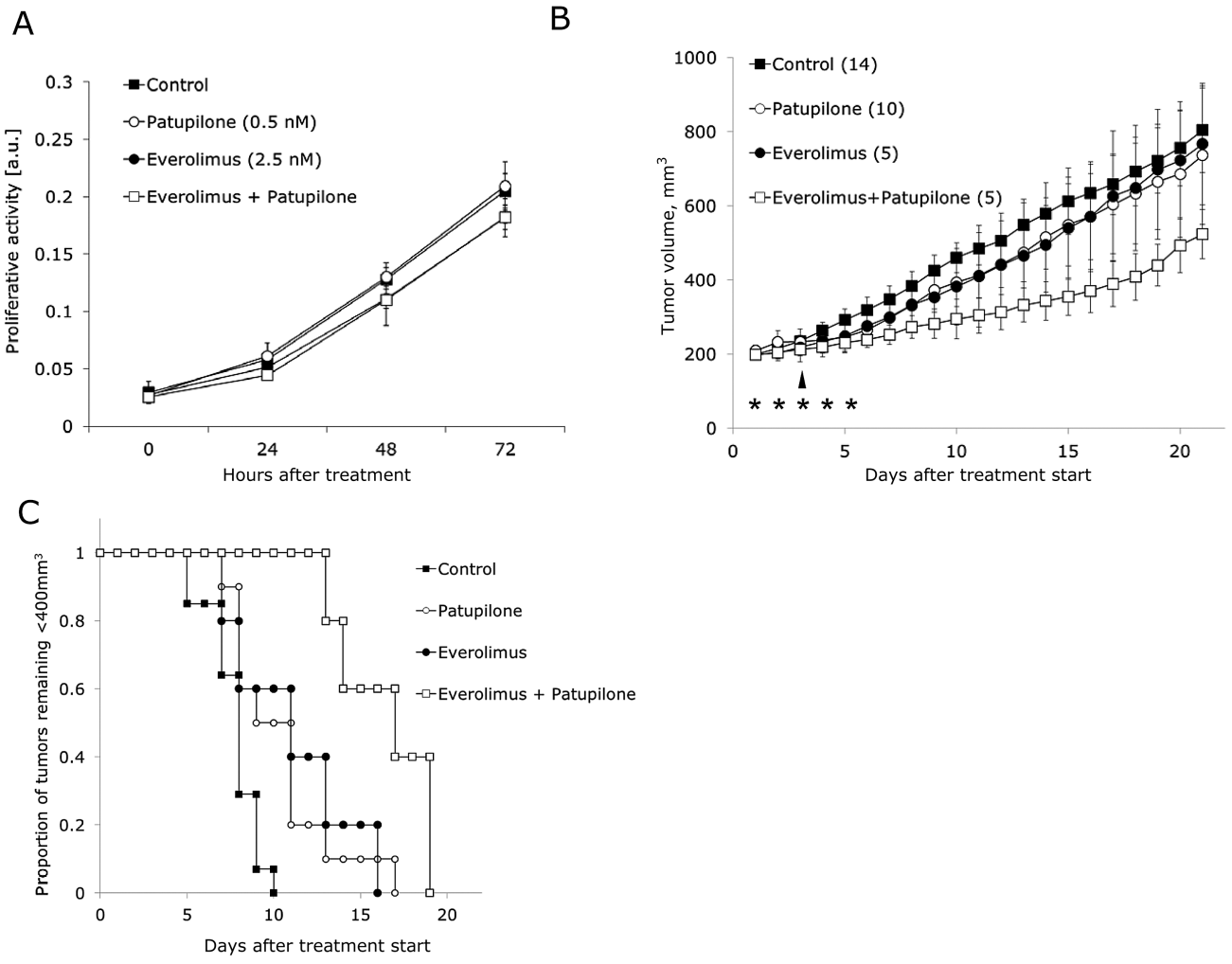

Figure 2. Combined treatment of patupilone-resistant lung adenocarcinoma cells and tumor xenografts with patupilone and everolimus. **A)** Antiproliferative effect of patupilone (0.5 nM) and everolimus (2.5 nM) in vitro. Data are means from three independent experiments. **Error bars** represent standard deviations. **B)** Tumor growth delay of A549EpoB40-derived tumor xenografts (5–14 per group, as indicated in the figure) in response to combined treatment with patupilone (2 mg/kg, one application) and everolimus (2.5 mg/kg, during five consecutive days). **Error bars** represent standard deviations. *P* values determined by two-sided analysis of variance using the Tukey Test for pair-wise comparisons. **C)** Kaplan-Meier curves for tumors reaching 400 mm^3 tumor volume. Tumor growth delays were calculated by Kaplan-Meier analysis with Holm-Sidak tests being used for pair-wise comparisons. All statistical tests were two-sided.

day 1, 4, and 7) induced a statistically significant reduction of tumor volume AUC (combined 8930 ± 921 vs control 12695 ± 2236, *P* = .016) (Figure 3B) in these tumors, as also observed for other tumor entities treated with such a minimal regimen of this antiangiogenic agent (33,34). Importantly, VEGF deprivation also sensitized for the MSA and combined treatment with patupilone resulted in an extended tumor growth delay in these otherwise patupilone-resistant tumors (AUC bevacicumab 8930 ± 921 vs bevacizumab plus patupilone 6453 ± 1580, *P* = .016; TGD, 400 mm^3, bevacicumab 15.8 ± 1.36 days vs bevacizumab plus patupilone 22.75 ± 1.63 days, *P* = .006) (Figure 3C). These results corroborate the results obtained by the combined treatment modality with everolimus and reinforce that tumor-derived survival factors, in particular VEGF, represent a major component of tumor resistance to MSAs.

To determine the potency and a putative antiangiogenic effect of the different treatment modalities in situ, microvessel density (MVD), the level of phosphorylated P70-S6Kinase, and the proliferative status (Ki-67/MIB-1-positive cells) were determined in histological tumor sections (Figure 4, A-C). Tumors were collected 24 hours after the last treatment with everolimus and bevacizumab alone or in combination with patupilone. The level of phosphorylated P70-S6Kinase was reduced in response to everolimus (32.33 ± 3.05 positive cells/visual field) by 65% in comparison with untreated control tumors (61.10 ± 2.20 positive cells/visual field), demonstrating the potency of the mTOR inhibitor (*P* = .001). The level of phosphorylated P70-S6kinase was not statistically significantly affected by cotreatment with patupilone or by treatment with patupilone alone, and, as expected, neither by bevacizumab nor by bevacizumab in combination with patupilone (Figure 4A). The proliferative activity of the MSA-resistant tumors was not reduced by patupilone. On the other hand, all other treatment modalities statistically significantly reduced the proliferative activity to comparable extents, which corresponds to the antiproliferative activity of most of these treatment modalities at this early time point after treatment start (*P* < .001) (Figure 4C). Interestingly, the microvessel density was strongly reduced down to 37% and 30% of control, when patupilone was used in combination with everolimus and bevacizumab, respectively (control 44.8 ± 8.4 MV/visual field vs patupilone plus everolimus 17.3 ± 2.3 MV/visual field,

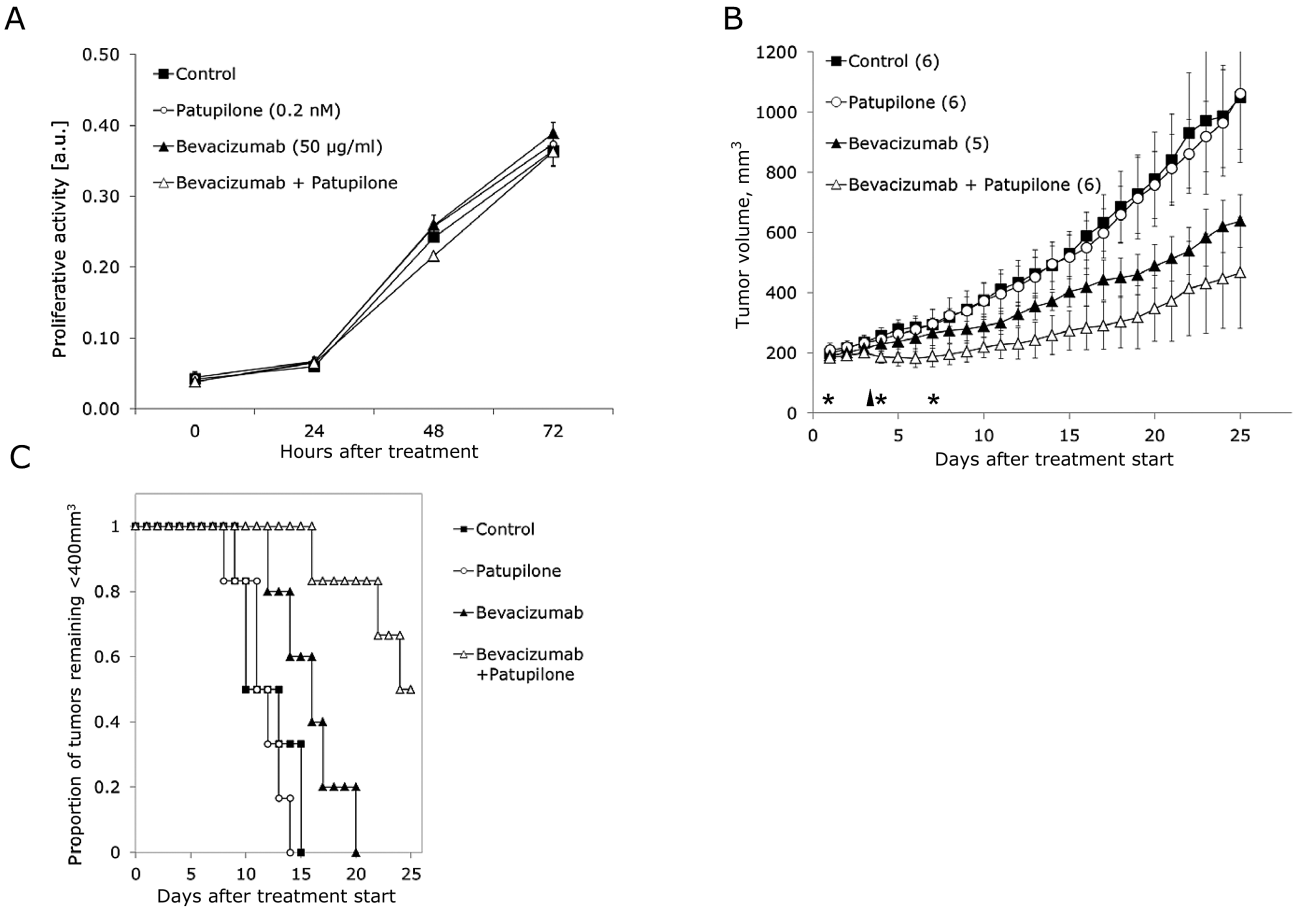

Figure 3. Combined treatment of patupilone-resistant lung adenocarcinoma cells and tumor xenografts with patupilone and bevacizumab. **A)** Antiproliferative effect of patupilone (0.2 nM) and bevacizumab (50 µg/mL) in vitro. Data are means from three independent experiments. **Error bars** represent standard deviations. **B)** Tumor growth delay of A549EpoB40-derived tumor xenografts (n = 5–6 per group) in response to combined treatment with patupilone (2 mg/kg, one application) and bevacizumab (3x10 mg/kg). **Error bars** represent standard deviations. *P* values were determined by two-sided analysis of variance using the Tukey Test for pair-wise comparisons. **C)** Kaplan-Meier curves for tumors reaching 400 mm^3 tumor volume. Tumor growth delays were calculated by Kaplan-Meier analysis with Holm-Sidak tests being used for pair-wise comparisons All statistical tests were two-sided.

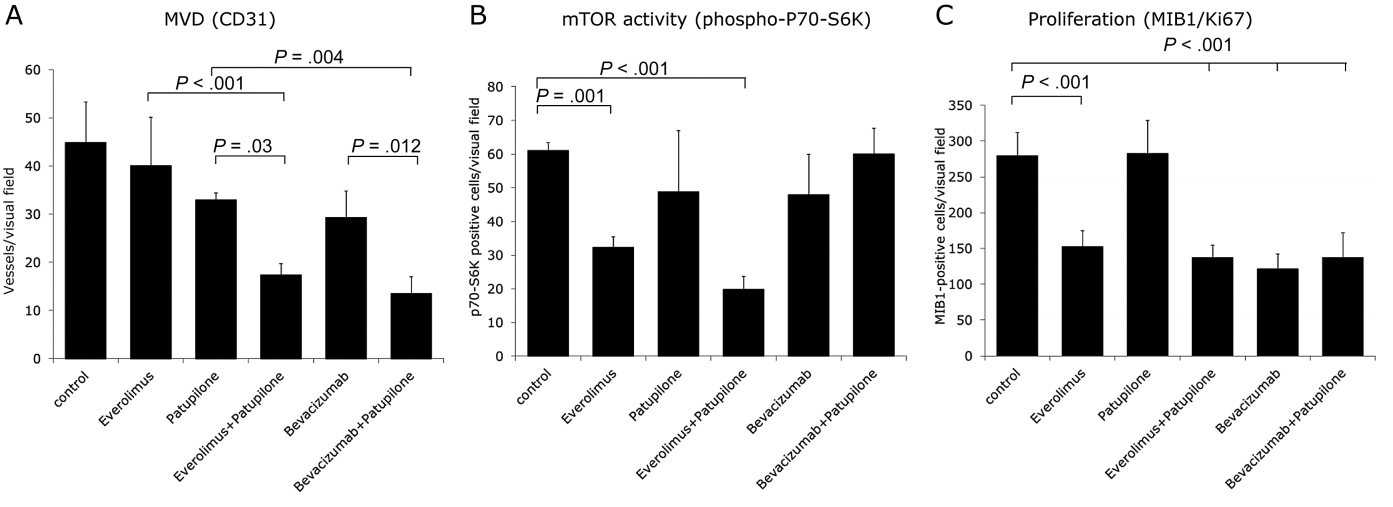

Figure 4. Response to treatment with patupilone, everolimus, and bevacizumab alone and in combination. **A)** Microvessel density. **B)** mTOR activity. **C)** Tumor cell proliferation. Mice carrying A549EpoB40-derived xenografts (n = 3 per group) were treated as described, and tumors were collected 24 hours after the last treatment with everolimus and bevacizumab alone or in combination with patupilone. Tumors from patupilone alone–treated mice were collected 24 hours after the last dose of the corresponding combined treatment modality. Tumors were harvested, formalin fixed and stained for CD31, phospho-P70-S6Kinase, and MIB1/Ki-67. **Error bars** represent standard deviations. Data were analyzed by one-way analysis of variance on replicate tumor samples (n = 6–9), and pair-wise analysis was performed using the Tukey Test. Relevant comparisons are given in the text and figures. All statistical tests were two-sided. MVD = microvessel density.

P = .03; patupilone plus bevacizumab 13.5 ± 3.5 MV/visual field, P = .004) (Figure 4A). Strong morphological changes with almost crumbled and destructed vessels were only observed in response to the combined treatment modalities (patupilone plus everolimus and patupilone plus bevacizumab, respectively). Representative tumor sections depict microvessel density, mTOR activity and tumor cell proliferation in response to treatment (Figure 5). These results suggest a positive antiangiogenic interaction between the MSA and everolimus and bevacizumab, respectively, in these MSA-resistant tumors. Additional in vitro experiments also demonstrated a VEGF-protective effect on endothelial cells towards patupilone. Pretreatment of endothelial cells with bevacizumab again resensitized these cells to the MSA (Supplementary Figure 2, available online).

Effect of Paclitaxel, Bevacizumab, and Combined Treatment on Growth of PgP-Overexpressing SW480-Derived Tumor Xenografts

While A549EpoB40 cells carry a specific mutation in the MSA-binding region of β-tubulin, leading to patupilone and taxane resistance, many tumors overexpress the multidrug resistance (MDR)–related efflux pump P-glycoprotein, thereby strongly reducing the potency of P-glycoprotein substrates such as taxanes (35). We probed the strategy to combine MSAs with inhibitors of angiogenesis also in a carcinoma tumor model (SW480), which is MSA resistant because of PgP-overexpression (31). Control in vitro experiments confirmed that these colon adenocarcinoma cells are completely resistant to paclitaxel and bevacizumab (Figure 6A). SW480-derived tumor xenografts were completely resistant to treatment with paclitaxel alone (20 mg/kg, day 3) while bevacizumab (2x5 mg/kg, day 1 and 4) induced a partial tumor growth delay (to double tumor volume control 10.60 ± 1.70 days vs bevacizumab 15.80 ± 2.71 days, P = .003). Similar to the treatment response observed in the lung carcinoma tumor model (see above), a combined treatment modality of paclitaxel in combination with bevacizumab also induced a statistically significant tumor growth delay in this otherwise paclitaxel-resistant tumor model (bevacizumab 15.80 ± 2.71 days vs bevacizumab plus paclitaxel 24.4 ± 5.28 days, P = .013). Tumors did not even double their tumor volume over the entire observation time of 25 days in response to this minimal combined treatment regimen (Figure 6, B and C). A comparable strong treatment response was observed when tumors were treated with a different treatment regimen of bevacizumab (1x10 mg/kg) in combination with paclitaxel (20 mg/kg) (see Supplementary Figure 3, available online). These results, obtained in a β-tubulin-mutation-unrelated, additional MSA–resistant tumor model, confirm the potency of a combined treatment modality of MSA and inhibitors of angiogenesis against otherwise MSA-refractory tumors.

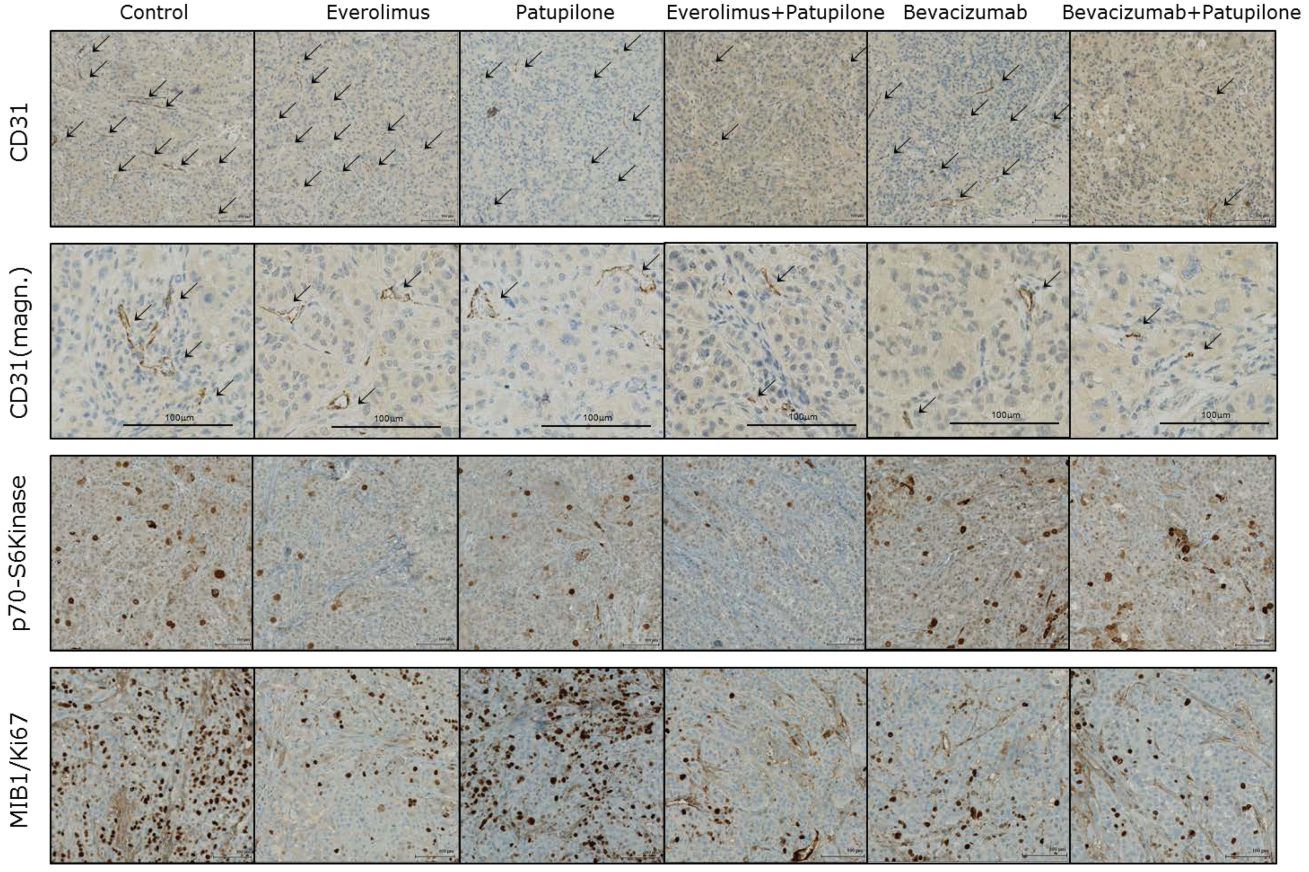

Figure 5. Representative tumor sections depicting microvessel density, high magnification images of representative vessels, mTOR activity, and tumor cell proliferation in response to treatment. Mice carrying A549EpoB40-derived xenografts (n = 3 per group) were treated as described, and tumors were collected 24 hours after the last treatment with everolimus and bevacizumab alone or in combination with patupilone. Tumors from patupilone alone–treated mice were collected 24 hours after the last dose of the corresponding combined treatment modality. Tumors were harvested, formalin fixed and stained for CD31, phospho-P70-S6Kinase, and MIB1/Ki-67. **Arrows** indicate microvessels. **Scale bars** for all pictures correspond to 100 µm.

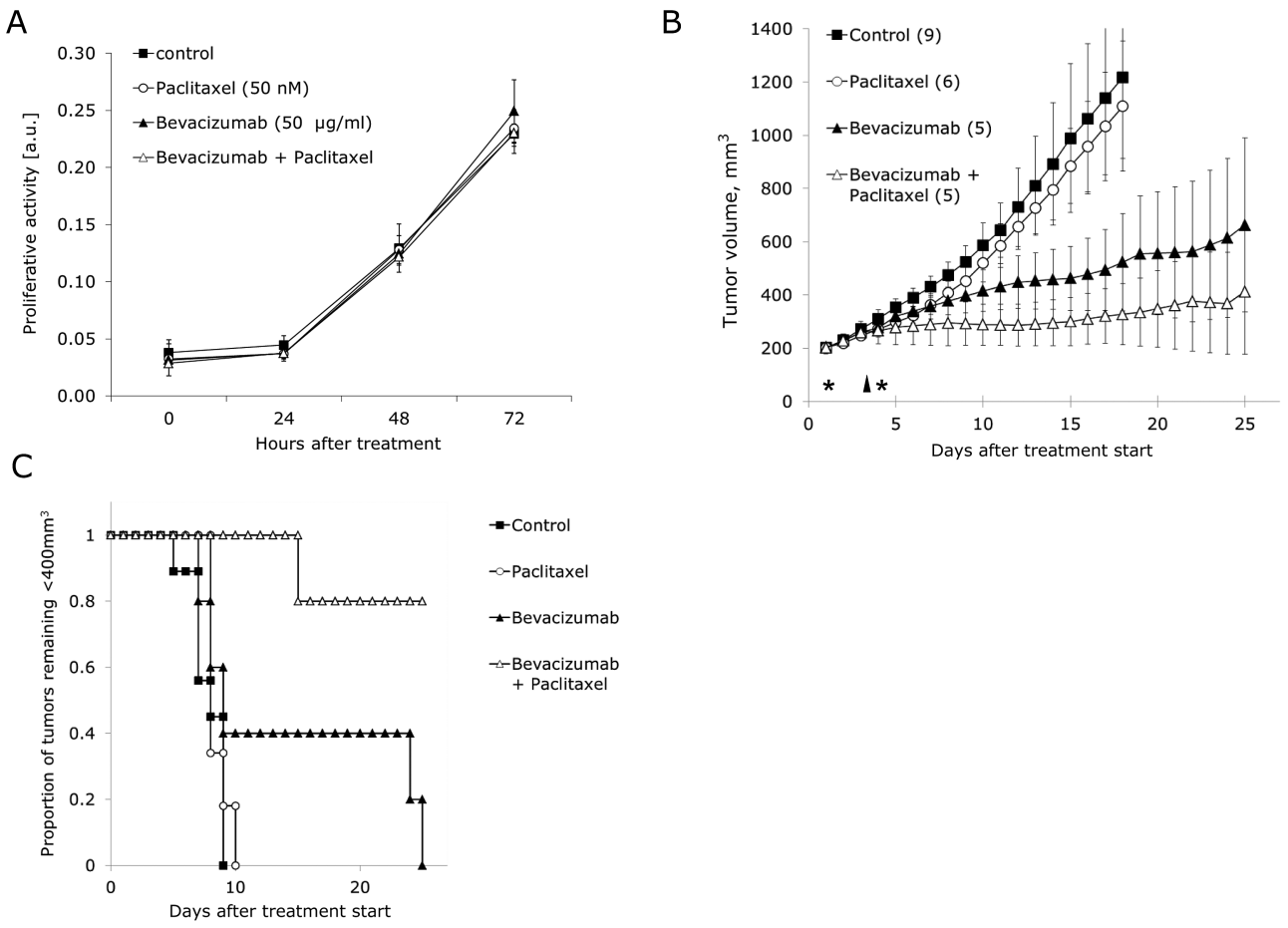

Figure 6. Combined treatment of paclitaxel-resistant SW480 colon adenocarcinoma cells and tumor xenografts with patupilone and bevacizumab. **A)** Antiproliferative effect of paclitaxel (50 nM) and bevacizumab (50 µg/mL) in vitro. Data are means from three independent experiments. **Error bars** represent standard deviations. **B)** Tumor growth delay of SW480-derived tumor xenografts (n = 5–9 per group) in response to combined treatment with paclitaxel (20 mg/kg, one application) and bevacizumab (2x5 mg/kg). **Error bars** represent standard deviations. *P* values were determined by two-sided analysis of variance using the Tukey Test for pair-wise comparisons. **C)** Kaplan-Meier curves for tumors reaching 400 mm^3 tumor volume. Tumor growth delays were calculated by Kaplan-Meier analysis with Holm-Sidak tests being used for pair-wise comparisons. All statistical tests were two-sided.

ARTICLE

Discussion

Resistance to microtubule-stabilizing agents is a major hurdle for successful cancer therapy. MSAs have a tumor cell–directed but also a major tumor vasculature–directed effect. Our own previous and novel results have demonstrated that potent antivascular targeting still depends on the interference of MSAs with the functional microtubular network in tumor cells (15,23). Intrinsic or acquired cell resistance to MSAs on the tumor cell level subsequently also abrogates its antivascular potency. Therefore, a combined treatment modality of MSA with an antiangiogenic, VEGF-reducing agent could overcome a tumor cell–based intrinsic MSA resistance in vivo and reestablish its potent antivascular effect.

We mechanistically investigated this concept in two tumor models that are MSA resistant either because of a tumor cell–specific β-tubulin mutation or the overexpression of the multidrug resistance–related efflux pump P-glycoprotein. Tubulin mutations and PgP overexpression are both of clinical relevance and hamper the broader use of MSAs as a first-line therapeutic option, eg, for MDR-overexpressing colon carcinoma or for metastatic breast cancer. We previously determined that a combined treatment modality of patupilone with a broad-range cytotoxic agent could not overcome patupilone resistance in these highly MSA-resistant tumors. Interestingly, we now demonstrate that specific downregulation of proangiogenic VEGF signaling by mTOR inhibition or VEGF neutralization with clinically approved agents strongly resensitizes these patupilone-resistant lung-adenocarcinoma cell-derived tumors to patupilone. Likewise taxane-resistant colon carcinomas, which are MDR overexpressing, were resensitized upon VEGF deprivation. A combined treatment modality of taxane with the mTOR inhibitor everolimus was not investigated in the colon carcinoma tumor model since everolimus is also a substrate for the P-glycoprotein efflux pump (36). Our own in vitro results corroborated that everolimus is a P-glycoprotein substrate (Supplementary Figure 4, available online).

Several preclinical studies have reported on the promising combined treatment of MSAs with mTOR inhibitors, and enhanced activity could be linked to increased tumor cell apoptosis. However, these studies and combined treatment modalities including MSAs with bevacizumab were solely performed in tumor cell systems and tumor xenografts that were already responsive to patupilone or taxanes alone and were not characterized as MSA refractory. Likewise, several clinical trials were conducted with related combined treatment modalities against multiple tumor entities and demonstrated feasibility with promising activity, but none of these trials stratified along known MSA resistances (25,28,30). In particular, the efficacy of paclitaxel plus

bevacizumab was compared with paclitaxel alone for metastatic breast cancer and revealed prolonged progression-free survival (primary endpoint) but not overall survival. However, this phase III trial also did not stratify for MSA resistances (30). Resensitization by the antiangiogenic agent might only manifest in MSA-resistant but not in MSA-responsive cases. Likewise we could not observe enhanced potency of the combined treatment modality (patupilone with everolimus) in patupilone-sensitive tumor xenografts. Interestingly, a case study has recently reported on resensitization of a paclitaxel-resistant metastatic breast cancer patient to paclitaxel therapy by additional bevacizumab treatment, supporting the results investigated in our study (37).

The strong treatment responses to a minimal combined treatment regimen of MSAs with bevacizumab in otherwise patupilone- and paclitaxel- completely refractory tumors mechanistically demonstrate that indeed VEGF as survival factor abrogates the primarily antivascular-directed and eventually strong tumor controlling effect of MSAs. In tumors derived from patupilone- and paclitaxel-sensitive tumor cells, the MSAs successfully diminish VEGF secretion by microtubule interference and thereby prime the tumor for their antivasculature activity on their own. Our immunohistochemical analysis further supports that the combined treatment modality initially affects the tumor vasculature. It is primarily the microvessel density and not the proliferative activity of tumor cells that is initially reduced upon combined treatment in tumor xenografts derived from MSA-resistant tumor cells.

This study also had some limitations. As efficacy-oriented endpoints we determined increase of tumor volume over time and absolute tumor growth delay in response to treatment, complemented by relevant mechanistic experiments. Tumor control as an additional efficacy-oriented endpoint could further illustrate the potency of these combined treatment modalities to overcome MSA resistances. Furthermore it will be of interest to validate this treatment modality also in orthotopic MSA-resistant tumor models, thereby identifying also putative additional microenvironmental factors that might codetermine treatment outcome.

Overall, our results demonstrate that the interaction between the tumor cell compartment and the tumor microenvironment strongly determines the treatment response to different microtubule-stabilizing agents. More important, a combined treatment modality of MSAs with antiangiogenic agents could overcome tumor cell–linked MSA resistance and should be further considered as clinical strategy for MSA-refractory tumor entities with intrinsic or acquired resistance mechanisms.

Funding

This work was supported in part by grants from the Swiss Cancer League (KLS-02788-02-2011), the Swiss National Science Foundation (144060), the Vontobel Stiftung, the Fonds für Medizinische Forschungen, and the KFSP Tumor Oxygenation of the University of Zurich.

Notes

Abstracts of this paper were already been presented at several conferences: the ICTR-PHE 2014 Conference, Geneva, CH, February 10 to 14, 2014, the 13 Int. Wolfsberg Meeting on Molecular Radiation Oncology, Ermatingen, CH, June 22 to 24, 2013.

These sponsors did not have a role in the design of the study, the collection, analysis or interpretation of the data, the writing of the manuscript, nor the decision to submit the manuscript for publication.

We thank Martina Storz (Deptartment of Pathology, University Hospital Zurich) for excellent technical support and the Biologisches Zentrallabor of the University Hospital of Zurich for animal housing.

References

1. Bollag DM, McQueney PA, Zhu J, et al. Epothilones, a new class of microtubule-stabilizing agents with a taxol-like mechanism of action. *Cancer Res*. 1995;55(11):2325–2333.
2. Kowalski RJ, Giannakakou P, Hamel E. Activities of the microtubule-stabilizing agents epothilones A and B with purified tubulin and in cells resistant to paclitaxel (Taxol(R)). *J Biol Chem*. 1997;272(4):2534–2541.
3. Manfredi JJ, Parness J, Horwitz SB. Taxol binds to cellular microtubules. *J Cell Biol*. 1982;94(3):688–696.
4. Schiff PB, Horwitz SB. Taxol stabilizes microtubules in mouse fibroblast cells. *Proc Natl Acad Sci U S A*. 1980;77(3):1561–1565.
5. Sparano JA. Taxanes for breast cancer: an evidence-based review of randomized phase II and phase III trials. *Clin Breast Cancer*. 2000;1(1):32–40; discussion 41–42.
6. Bonomi P, Kim K, Fairclough D, et al. Comparison of survival and quality of life in advanced non-small-cell lung cancer patients treated with two dose levels of paclitaxel combined with cisplatin versus etoposide with cisplatin: results of an Eastern Cooperative Oncology Group trial. *J Clin Oncol*. 2000;18(3):623–631.
7. Altmann KH, Gertsch J. Anticancer drugs from nature--natural products as a unique source of new microtubule-stabilizing agents. *Nat Prod Rep*. 2007;24(2):327–357.
8. He L, Yang CP, Horwitz SB. Mutations in beta-tubulin map to domains involved in regulation of microtubule stability in epothilone-resistant cell lines. *Mol Cancer Ther*. 2001;1(1):3–10.
9. Nogales E. Structural insights into microtubule function. *Annu Rev Biochem*. 2000;69:277–302.
10. Altmann KH, Wartmann M, O'Reilly T. Epothilones and related structures--a new class of microtubule inhibitors with potent in vivo antitumor activity. *Biochim Biophys Acta*. 2000;1470(3):M79–M91.
11. Stein A. Ixabepilone. *Clin J Oncol Nurs*. 2010;14(1):65–71.
12. Raspaglio G, Filippetti F, Prislei S, et al. Hypoxia induces class III beta-tubulin gene expression by HIF-1alpha binding to its 3' flanking region. *Gene*. 2008;409(1–2):100–108.
13. Kavallaris M. Microtubules and resistance to tubulin-binding agents. *Nat Rev Cancer*. 2010;10(3):194–204.
14. Kavallaris M, Kuo DY, Burkhart CA, et al. Taxol-resistant epithelial ovarian tumors are associated with altered expression of specific beta-tubulin isotypes. *J Clin Invest*. 1997;100(5):1282–1293.
15. Bley CR, Jochum W, Orlowski K, et al. Role of the microenvironment for radiosensitization by patupilone. *Clin Cancer Res*. 2009;15(4):1335–1342.
16. Bocci G, Nicolaou KC, Kerbel RS. Protracted low-dose effects on human endothelial cell proliferation and survival in vitro reveal a selective antiangiogenic window for various chemotherapeutic drugs. *Cancer Res*. 2002;62(23):6938–6943.
17. Ferretti S, Allegrini PR, O'Reilly T, et al. Patupilone induced vascular disruption in orthotopic rodent tumor models detected by magnetic resonance imaging and interstitial fluid pressure. *Clin Cancer Res*. 2005;11(21):7773–7784.
18. Pasquier E, Carre M, Pourroy B, et al. Antiangiogenic activity of paclitaxel is associated with its cytostatic effect, mediated by the initiation but not completion of a mitochondrial apoptotic signaling pathway. *Mol Cancer Ther*. 2004;3(10):1301–1310.
19. Stalder MW, Anthony CT, Woltering EA. Metronomic dosing enhances the anti-angiogenic effect of epothilone B. *J Surg Res*. 2011;169(2):247–256.
20. Escuin D, Kline ER, Giannakakou P. Both microtubule-stabilizing and microtubule-destabilizing drugs inhibit hypoxia-inducible factor-1alpha accumulation and activity by disrupting microtubule function. *Cancer Res*. 2005;65(19):9021–9028.
21. Furmanova-Hollenstein P, Broggini-Tenzer A, Eggel M, et al. The microtubule stabilizer patupilone counteracts ionizing radiation-induced matrix metalloproteinase activity and tumor cell invasion. *Radiat Oncol*. 2013;8:105.
22. Orlowski K, Rohrer Bley C, Zimmermann M, et al. Dynamics of tumor hypoxia in response to patupilone and ionizing radiation. *PLoS One*. 2012;7(12):e51476.
23. Rohrer Bley C, Orlowski K, Furmanova P, et al. Regulation of VEGF-expression by patupilone and ionizing radiation in lung adenocarcinoma cells. *Lung Cancer*. 2011;73(3)294–301..
24. Faried LS, Faried A, Kanuma T, et al. Inhibition of the mammalian target of rapamycin (mTOR) by rapamycin increases chemosensitivity of CaSki cells to paclitaxel. *Eur J Cancer*. 2006;42(7):934–947.
25. Hurvitz SA, Dalenc F, Campone M, et al. A phase 2 study of everolimus combined with trastuzumab and paclitaxel in patients with HER2-overexpressing advanced breast cancer that progressed during prior trastuzumab and taxane therapy. *Breast Cancer Res Treat*. 2013;141(3):437–446.
26. Mondesire WH, Jian W, Zhang H, et al. Targeting mammalian target of rapamycin synergistically enhances chemotherapy-induced cytotoxicity in breast cancer cells. *Clin Cancer Res*. 2004;10(20):7031–7042.

27. O'Reilly T, McSheehy PM, Wartmann M, et al. Evaluation of the mTOR inhibitor, everolimus, in combination with cytotoxic antitumor agents using human tumor models in vitro and in vivo. *Anticancer Drugs*. 2011;22(1):58–78.
28. Sun JM, Kim JR, Do IG, et al. A phase-1b study of everolimus plus paclitaxel in patients with small-cell lung cancer. *Br J Cancer*. 2013;109(6):1482–1487.
29. Zhou Q, Wong CH, Lau CP, et al. Enhanced Antitumor Activity with Combining Effect of mTOR Inhibition and Microtubule Stabilization in Hepatocellular Carcinoma. *Int J Hepatol*. 2013;2013:103830.
30. Miller K, Wang M, Gralow J, et al. Paclitaxel plus bevacizumab versus paclitaxel alone for metastatic breast cancer. *N Engl J Med*. 2007;357(26):2666–2676.
31. Hofstetter B, Vuong V, Broggini-Tenzer A, et al. Patupilone acts as radiosensitizing agent in multidrug-resistant cancer cells in vitro and in vivo. *Clin Cancer Res*. 2005;11(4):1588–1596.
32. Lane HA, Wood JM, McSheehy PM, et al. mTOR inhibitor RAD001 (everolimus) has antiangiogenic/vascular properties distinct from a VEGFR tyrosine kinase inhibitor. *Clin Cancer Res*. 2009;15(5):1612–1622.
33. Jin K, Lan H, Cao F, et al. Differential response to EGFR- and VEGF-targeted therapies in patient-derived tumor tissue xenograft models of colon carcinoma and related metastases. *Int J Oncol*. 2012;41(2):583–588.
34. Zhou F, Hu J, Shao JH, et al. Metronomic chemotherapy in combination with antiangiogenic treatment induces mosaic vascular reduction and tumor growth inhibition in hepatocellular carcinoma xenografts. *J Cancer Res Clin Oncol*. 2012;138(11):1879–1890.
35. Mickisch GH, Licht T, Merlino GT, et al. Chemotherapy and chemosensitization of transgenic mice which express the human multidrug resistance gene in bone marrow: efficacy, potency, and toxicity. *Cancer Res*. 1991;51(19):5417–5424.
36. Laplante A, Demeule M, Murphy GF, et al. Interaction of immunosuppressive agents rapamycin and its analogue SDZ-RAD with endothelial P-gp. *Transplant Proc*. 2002;34(8):3393–3395.
37. Ishizuna K, Ninomiya J, Kojima M, et al. Paclitaxel-resistant advanced recurrent breast cancer: a case of partial response because of addition of bevacizumab to paclitaxel therapy: a case report. *BMC Res Notes*. 2013;6(1):254.